On the modeling of thermo-mechanical concrete for the finite element analysis of structures submitted to elevated temperatures

W.Nechnech & J.M.Reynouard
URGC-Structures, Institut National des Sciences Appliquées de Lyon, France

F.Meftah
Laboratoire Génie Civil et Urbanisme, Université de Marne La Vallée, France

ABSTRACT: In this paper a thermo-plastic damage model for plain concrete subjected to combined thermal and cyclic loading is developed using the concept of plastic-work-hardening and stiffness degradation in continuum damage mechanics. Two damage variables are used, one for mechanical action and the other for thermal one. The concrete model is based on the non-associated flow theory of plasticity with a scalar hardening parameter, a multi-criteria yield function. Further, thermo-mechanical interaction strains have been introduced to describe the influence of mechanical loading path on the physical process of thermal expansion of concrete. The constitutive relations for elastoplastic response are decoupled with the degradation damage response by using the effective stress concept. The Efficiency of the proposed thermo-plastic damage model is demonstrated through numerical examples with the experimental counterparts.

1 INTRODUCTION

The evaluation of the residual strength of structural components that have been damaged during their service life has become imperative for modern civil engineering. In particular, the assessment of severe accidental situations such as nuclear disease or fire is of prime practical importance processes (Baker and Stabler 1999; Heinfling 1998).

The need to design durable concrete structures, leads ever more to sophisticated modeling of deterioration phenomena. Thus, it is essential to consider the coupling and the non linearity of the all the processes involved in the degradation mechanisms. At the structural scale, elevated temperatures induce restrained thermal dilatation due to kinematic constraints. Therefore, self equilibrated stresses do rise and combine with stresses due to mechanical loads to drive cracks. At the material scale, thermal load induces strong micro-structural changes that alter the mechanical behaviour of concrete: loss of stiffness and strength of the material. This degradation results mainly from the dehydration of concrete on the micro-level. It may also results from the difference in thermal dilatation coefficient between the aggregates and the cement paste, in particular in concrete with silicious aggregates. Further, the low permeability of concrete induces pressure build up that leads to a significant degradation of the material and therefore of its carrying capacity.

This paper focused on damaging processes in concrete ascribed to both combined mechanical loads and transient high temperature distribution. The phenomenological behavior of concrete at the macroscopic level is modelled by a coupled elastoplastic damage approach in which the effective stress concept has been introduced (Kachanov 1986). Two scalar damage variables are introduced in the relationship between the stresses and the effective stresses. A thermal damage variable describes stiffness degradation due to diffused thermal isotropic cracking. A mechanical damage variable describes stiffness degradation process due to more localized mechanical cracking process when the carrying capacity of the material decreases with temperature. These two processes of degradation are considered to be independent. In this model, the evolution of the mechanical damage variable is related to the physically observed crack opening represented by the plastic strain. This makes it convenient to calibrate the damage evolution from experimental results naturally based on the stress, without introducing an additional damage surface based on the strain. Furthermore, it is well known that when loading ranges between the tensile and the compressive states, the recovery of degraded stiffness is observed during unloading from the tensile region to the compressive region (Reinhardt 1984). The stiffness recovery is a consequence of the closing of the previously opened cracks. The mechanical damage variable is then subdivided in two parts, one for tensile loading and the other for compressive one. This provides the separate evolution of the directional damage and then allows capturing stiffness recovery. This concrete model is also based on the non-associated flow theory of plasticity with a scalar hardening parameter. A

multi-surfaces criterion is used to describe the induced anisotropy.

Moreover, thermo-mechanical modelling of concrete should take into account thermal transient creep. This phenomenon has been carried out by Anderberg and Thelandersson (1976). In the experiment, a reversal of the sequence of applied stress and temperature fields yielded tensile strains when temperature was applied first, but compressive strains when loaded first. Indeed, creep strain appears due to compressive stress and is amplified by increasing temperature. The elaborated model does incorporate this additional thermo-mechanical interaction strain component.

The Efficiency of the proposed thermo-plastic damage model is demonstrated through numerical examples with the experimental counterparts.

2 BASIC EQUATIONS

The equilibrium and the heat process, in the considered thermo-mechanical coupled problems, are governed by the two following set of equations in which the dote represents derivation with respect to time,

$$div(\sigma) = \mathbf{0}$$
$$\rho \cdot \dot{e} = \sigma : \dot{\varepsilon} - div(\mathbf{q}) \tag{1}$$

where σ is the stress tensor, ε the strain tensor, $\dot{e}$ the density of internal energy rate, ρ the masse density and $\mathbf{q}$ the heat flux vector given by Fourier's low

$$\mathbf{q} = -\lambda \, grad\theta \tag{2}$$

where λ is the conductivity coefficient of heat whose aim to account for thermo-mechanical degradation due to increase of porosity.

In order to model isotropic phenomena of thermo-plastic and damage within the framework of irreversible processes of thermodynamics, a set of state variables is used. The Helmholtz free energy density Ψ is then considered as the thermodynamic potential, which is a convex function of all the state variables

$$\Psi = \Psi_e(\varepsilon^e, \theta, D, \Lambda) + \Psi_p(\kappa, \Lambda) \tag{3}$$

and is linked to the density of internal energy given in Eq. 1 by

$$e = \Psi + \theta \cdot \eta \tag{4}$$

where θ is the absolute temperature and η is the entropy. In Eq. 3, Ψ_e denotes the elastic free energy of the material

$$\Psi_e(\varepsilon^e, \theta, D, \Lambda) = \frac{1}{2}\varepsilon^e : \mathbf{E} : \varepsilon^e - \vartheta \, \mathbf{K} : \varepsilon^e - \frac{1}{2}C\frac{\vartheta^2}{\theta_0} \tag{5}$$

in which C is the specific heat and θ_0 the initial temperature of the system. The current material stiffness tensor $\mathbf{E}$ and the second order symmetric coupling tensor $\mathbf{K}$ are given by

$$\mathbf{E} = (1 - D)(1 - \Lambda)\mathbf{E}_0, \quad \mathbf{K} = 3K\alpha \cdot \mathbf{1} \tag{6}$$

where $\mathbf{E}_0$ is the initial stiffness tensor, K the bulk modulus, α the coefficient of thermal expansion and $\mathbf{1}$ the unite tensor. The independent state variables are therefore the elastic strain ε^e, the relative temperature $\vartheta = \theta - \theta_0$, the mechanical damage variable D and the thermal damage variable Λ.

Furthermore, Ψ_p is the plastic free energy in which the internal state variable κ is the hardening parameter that controls the plastic process. The assumption of uncoupling between reversible and irreversible processes has been made. The total strain tensor ε is therefore decomposed to an elastic part ε^e, plastic part ε^p and thermal part ε^θ as

$$\varepsilon = \varepsilon^e + \varepsilon^p + \varepsilon^\theta \tag{7}$$

Moreover, the hardening parameter κ can be defined as the cumulated plastic strain given by

$$\dot{\kappa} = \sqrt{(2/3)\dot{\varepsilon}^p : \dot{\varepsilon}^p} \tag{8}$$

3 DAMAGE EVOLUTION

The damage variable, associated to mechanical or thermal degradation processes of concrete, is interpreted as the surface density of materials defects (Kachanov 1958; Ju 1989), and will be defined as the ratio between the area occupied by created micro-cracks, overall material area. This definition states that damage variable is a non decreasing parameter, since the reduction of the effective resisting section area will continuously increase until failure occurs. The effect of thermal damage on concrete structures is a further decrease of the effective resisting area of a mechanical damaged material. The successive thermal damaging process, which is governed by the parameter Λ, will act on this area, and it is possible to define the coupled damage parameter d, which summarizes the coupling of both mechanical and thermal effects

$$d = 1 - (1 - D)(1 - \Lambda) \tag{9}$$

where D is the mechanical damage variable. Thus, the stress-strain relationship reads

$$\sigma = (1 - D)(1 - \Lambda)\mathbf{E}_0 : \varepsilon^e = \mathbf{E} : (\varepsilon - \varepsilon^p - \varepsilon^\theta)$$
$$\sigma = (1 - D)(1 - \Lambda)\tilde{\sigma} \tag{10}$$

where σ is the tensor of nominal stresses and $\tilde{\sigma}$ is the tensor of effective ones.

3.1 Mechanical damage variable

In the present analysis, we use an isotropic scalar damage model. The damage evolution law determines the global shape of the softening curve. The degree of brittleness of the mechanical effect of progressive micro-cracking due to external loads is described by a single internal scalar variable D which degrades the current Young's modulus of the material such that the stiffness tensor reads

$$\mathbf{E} = (1 - D)\mathbf{E}_0 \tag{11}$$

The damage evolution is considered as of an exponential form

$$1 - D_x = \exp(-c_x\,\kappa_x) \tag{12}$$

of the cumulated plastic strain, where c_x is a material parameter (Lee 1998; Meftah and al. 2000; Nechnech 2000). In order to describe different behavior in tensile (where subscript $x = t$) and compressive loading (where subscript $x = c$) observed in tests data, the mechanical damage variable is subdivided in two parts, one for tensile loading and the other for compressive one (Mazars 1984; Lee 1998). The modeling of the crack opening/closing behavior can be implemented by elastic-stiffness recovery during the elastic unloading process from tensile state to compressive state. Thus, the tensile damage variable is modified by a multiplying parameter p (Lee 1998; Nechnech 2000).

$$D(\kappa, \tilde{\sigma}) = 1 - (1 - D_c)(1 - p(\tilde{\sigma})D_t) \tag{13}$$

$$p(\tilde{\sigma}) = p_0 + (1 - p_0)\cdot\Omega(\tilde{\sigma})$$
$$\Omega(\tilde{\sigma}) = \sum_{i=1}^{i=3}\langle\tilde{\sigma}_i^p\rangle_+ \Big/ \sum_{i=1}^{i=3}|\tilde{\sigma}_i^p| \tag{14}$$

and $0 \le p_0 \le 1$. Here $\Omega(\sigma)$ is a scalar quantity, which represents a weight factor.

3.2 Thermal damage variable

In a similar way as for the mechanical damage, the thermal damage of heated concrete is described in terms of experimentally determined relations $E = E(\theta)$, which link the temperature θ to the current elastic modulus E. Then, combining this phenomenological relation, $E = E(\theta)$, with the relation $E = (1 - \Lambda)E_0$, one can determine the thermal damage function as

$$\Lambda(\theta) = 1 - \frac{E(\theta)}{E_0} \text{ with } \begin{cases} \dot{\Lambda} \ge 0 & \text{if } \dot{\theta} > 0 \\ \dot{\Lambda} = 0 & \text{else} \end{cases} \tag{15}$$

Note that the function $E(\theta)$ is obtained by compressive tests on specimens that have been heated at different temperatures and then cooled progressively in order to avoid additional degradation due to quick cooling.

4 COUPLING BETWEEN PLASTICITY AND DAMAGE

Once micro-cracks are initiated, local stresses are redistributed to undamaged material micro-bonds over the effective area. Thus, effective stresses of undamaged material points are higher than nominal stresses. Accordingly, it appears reasonable to state that the plastic flow occurs only in the undamaged material micro-bounds by means of effective quantities (Ju 1989). The plastic response is therefore characterized in the effective stress space and the yield surface is given by

$$F(\tilde{\sigma}, \kappa, \theta) \le 0 \tag{16}$$

In our model a non smooth multisurfaces criterion is used to describe the dissymmetrical material behavior in tension and compression of concrete (Feenstra 1993; Georgin 1998). The employed yield surfaces F_i are function of invariants of effective stress tensor $\tilde{\sigma}$, hardening parameter κ and temperature θ. For the tensile stress state, a Rankine yield function is used

$$F_t(\tilde{\sigma}, \kappa_t, \theta) = \tilde{\sigma}_I - \tilde{\tau}_t(\kappa_t, \theta) \tag{17}$$

and for the compressive stress state a Drucker-Prager one is used

$$F_c(\tilde{\sigma}, \kappa_c, \theta) = J_2(\tilde{s}) + \beta_1\,I_1(\tilde{\sigma}) - \beta_2\,\tilde{\tau}_c(\kappa_c, \theta) \tag{18}$$

where $\tilde{\sigma}_I$ is the major principal stress, $I_1(\tilde{\sigma})$ is the first invariant of the stress tensor, $J_2(\tilde{s})$ is the second invariant of the deviatoric stress tensor $\tilde{s}$, β_i $(i = 1, 2)$ are two multiplying factors and $\tilde{\tau}$ is the uniaxial equivalent effective stress in tension or in compression. The carrying capacity of the material given by the uniaxial equivalent effective stress $\tilde{\tau}$ is expressed by an analytically convenient function that may serve either in tensile case or compressive case. It is consistent with the fact that experimentally observed stress-strain curves tend to attain zero-stress level asymptotically. It may be defined by

$$\tilde{\tau}_x = \tau_x/(1 - d)$$
$$\tau_x = f_{x0}[(1 + a_x)\exp(-b_x\,\kappa_x) - a_x\exp(-2b_x\,\kappa_x)] \tag{19}$$

in which a_x and b_x are material parameters and f_{x0} is the initial tensile ($x = t$) or compressive ($x = c$) strength.

Furthermore, concrete is a frictional material whish makes necessary to adopt a non-associated plastic flow to control the dilatancy since the damage is

considered here as isotropic. A plastic potential is then introduced

$$\begin{cases} G_t = F_t \\ G_c = J_2(\widetilde{s}) + \beta_g \, I_1(\widetilde{\sigma}) - \beta_2 \, \widetilde{\tau}_c(\kappa, T) \end{cases} \tag{20}$$

where the parameter β_g is chosen to give proper dilatancy. The plastic strain rate tensor is then obtained by

$$\dot{\varepsilon}^p = \sum_{i=1}^{i=2} \dot{\lambda}_i \, \frac{\partial G_i}{\partial \widetilde{\sigma}} \tag{21}$$

where λ_i is the plastic multiplier associated to the plastic potential function G_i in tension or in compression.

5 THERMAL TRANSIENT CREEP

During first-time heating of a concrete specimen under sustained load, a significant increase in strains associated with the increase of temperature occurs. This phenomenon cannot be solely explained neither by the thermo-mechanical degradation of the elastic properties nor by the plastic flow. It has rather been linked to an additional strain component, which takes place in a very short period of time. This strain component, called transient thermo-mechanical interaction strain or transient creep strain, is considered as a function of the temperature as well as the stress. An excellent literature review on this subject was published Khoury and al. (1985). In their study Anderberg and Thelandersson (1976), proposed a simple one dimensional formula for the magnitude of the transient creep strain. This formula has been generalized to a multiaxial stress state by de Borst and Peeters (1989). Is has been successfully incorporated into a thermo plastic model by Khennane and Baker (1992) and by Heinfling and al. (1998). The proposed model for transient creep can be written as

$$\dot{\varepsilon}^{tm} = \dot{\theta} \, \mathbf{Q} : \widetilde{\sigma} \tag{22}$$

where $\mathbf{Q}$ is a fourth order tensor determined from transient creep tests.

$$Q_{ijkl} = \frac{\alpha \, \beta_0}{f_{c20}} \left\{ -\gamma \delta_{ij} \delta_{kl} + \frac{1}{2}(1+\gamma)\left(\delta_{ik}\delta_{jl} + \delta_{il}\delta_{jk}\right) \right\} \tag{23}$$

where (β_0, γ) are material parameters. The stress equation as gives by equation (10) for now becomes,

$$\sigma = \mathbf{E} : \left(\varepsilon - \varepsilon^p - \varepsilon^\theta - \varepsilon^{tm}\right) \tag{24}$$

6 NUMERICAL IMPLEMENTATION AND MODEL VALIDATION

An efficient numerical algorithm for the present model has been developed (Nechnech 2000) and implemented as a part of CASTEM2000 finite element code. The continuum tangent stiffness (Nechnech 2000) is used to maintain quadratic convergence rate in solving the nonlinear equations. In this section, several numerical examples of the present thermoplastic damage model for concrete are presented.

6.1 Cyclic loading test

To compare the present model with the existing experimental results (Karsan and Jirsa 1969 and; Gopalaratnam and Shah 1985), the following material properties are used.

Table 1. Mechanical material properties.

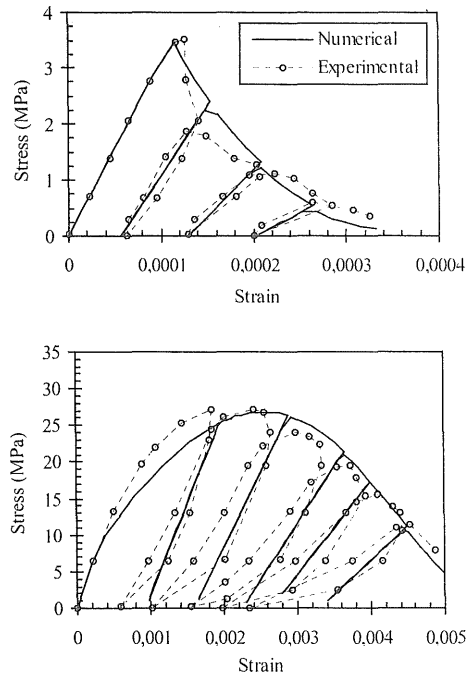|	Compressive test	tensile test
E_0 (N/mm^2)	31.7×10^3	31.0×10^3
ν	0.2	0.2
f_c (N/mm^2)	27.6	34.8
f_t (N/mm^2)	2.76	3.48
Model parameters	a_c=11.25	a_t=-0.5
	b_c=680	b_t=4046
	c_c=222.25	c_t=2419

Figure 1. Stress-strain behavior in cyclic tension (top) and cyclic compression (bottom) compared with experimental results.

Figure 1 (top), show the numerical result of a cyclic tensile loading test, and figure 1 (bottom), show the numerical result of a cyclic compressive loading test. subject to a cyclic loading in tensile and compressive case.

For both cases the degradation of stiffness is simulated at each unloading/reloading cycle as well as the softening behavior. The hysteresis on reloading cannot be simulated by the model.

6.2 *Thermal validation*

In this part, the constitutive responses of the model are simulated on specimens submitted to uniaxial tensile and compressive load at different temperatures, and therefore by focusing on the capability of the model to describe transient creep. At last a structural case is considered, in which a reinforced concrete slab is analyzed in a fire test.

6.2.1 *Uniaxial tensile and compressive tests*

Uniaxial compressive tests performed by Schneider (1988) and tensile tests performed by Felicetti and Gambrova (1998) on concrete specimens are simulated here. The simulated stress-strain curves are therefore compared to those given by the authors. In the considered experimental tests, the concrete specimen is submitted to a progressive temperature increase up to the desired value and then cooled slowly. After, the specimen is submitted to a compressive or tensile force in displacement control to get the stress-strain response.

The values of mechanical properties of the concrete at room temperature and their evolutions are given in Table 2 and in Table.3

Table 2. Mechanical properties of concrete for the compressive test.

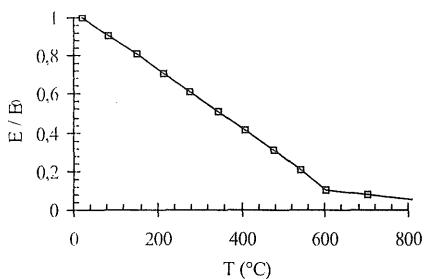| Values at room temperature		Variation with temperature
E_0 (N/mm^2)	29.6×10^3	Figure 2
ν	0.2	Constant
f_c (N/mm^2)	27.6	Figure 3
α (°C^{-1})	1.2×10^{-5}	Constant

Figure 2. Variation of elastic modulus with temperature.

The predicted stress-strain curves obtained with the present model are shown in Figure 6, together with the experimental curves for the temperatures reported by the authors (Schneider, 1988; Felicetti and
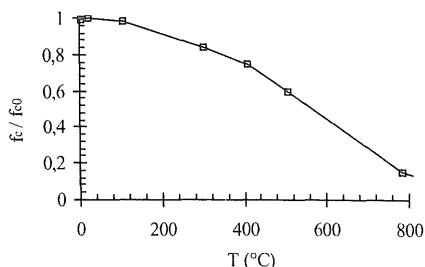

Figure 3. Variation of compressive strength with temperature.

Table 3. Mechanical properties of concrete for the tensile test.

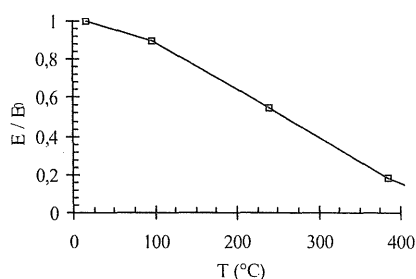| Values at room temperature		Variation with temperature
E_0 (N/mm^2)	50×10^3	Figure 4
ν	0.2	Constant
f_t (N/mm^2)	5.4	Figure 5
α (°C^{-1})	1.2×10^{-5}	Constant

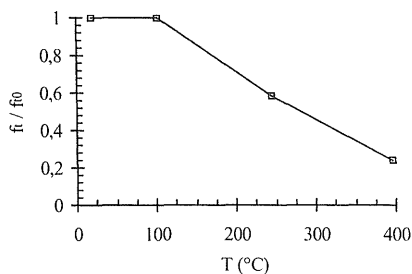Figure 4. Variation of elastic modulus with temperature.

Figure 5. Variation of tensile strength with temperature.

Gambrova 1998). The agreement between the predicted curves and the experimental ones is perfect. These results capture the main tends shown in the experimental data, namely the decrease of both the strength and the stiffness of the material, and also the variation of the brittleness of the softening behavior, which becomes more ductile when temperature increases. This is consistent with the observed experimental variation of the fracture energy (Nechnech 2000).
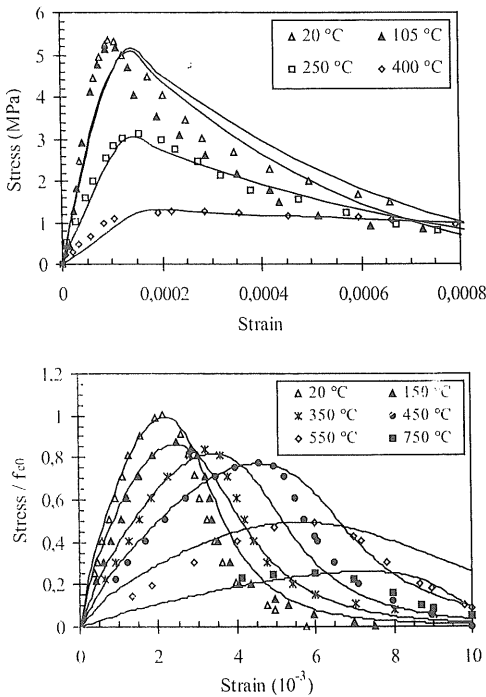
Figure 6. Stress-strain behavior in tension (top) and compression (bottom) at high temperatures compared with experimental results.

6.2.2 Transient creep test

To illustrate the influence of stress and temperature histories on the deformation behavior of concrete, the experiment conducted by Anderberg and Thelandersson (1976), is simulated. The specimens are heated under three constant stress levels: 22.5 %, 45.0 % and 67.5 % of the initial compressive strength f_{c0}. The transient creep parameters used in this test are $\beta_0 = 2.36$ and $\gamma = 0.20$.
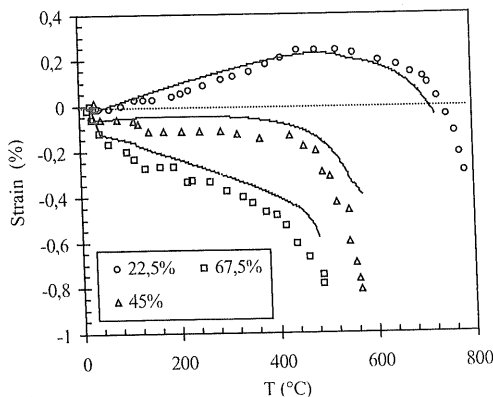

Figure 7. Deformation on heating under sustained load compared with experimental result.

The model prediction, together with the experimental response, is shown in figure 7. The agreement between the model and the experiment is good. Up to about 500°C, which corresponds to the yield temperature, the material response becomes elastoplastic due to thermal damage during heating, and the model predicts relatively well the failure of the specimen. Note that if the term of thermomechanical interaction strain has not been introduced in the constitutive model (Equation 24), the failure occurs earlier. This is due to an overestimation of the elastic strain and then of the stress which is not, in this case, relaxed by the additional term.

In order to carry out, once again, the importance that has the transient creep term, a further test taken from Anderberg and Thelandersson (1976) is simulated. The experiment consists in comparing the results obtained by two identical specimens. One specimen is first heated up to 400°C and, while temperature is kept constant, then is loaded axially at a constant stress level. The other specimen, however, is loaded first to the required stress and then heated up to 400°C.
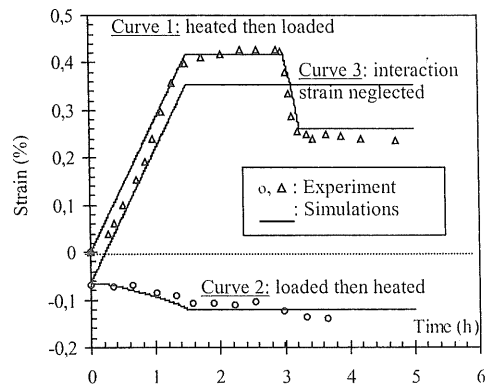

Figure 8. Strain response of concrete under two different load-temperature histories compared with experimental result.

Figure 8 represents the results of the simulation in both loading cases, together with the experimental ones. Curve 1 corresponds to the first case, while curve 2 corresponds to the second case. Simulation and experiment agree quite well in both cases when the themo-mechanical interaction term has been taken into account. However, the numerical result highlights a completely different path when this term is neglected, given by curve 3 in Fig.8, which is supposed to be similar to curve 2. These results validate the capacity of this model to describe the stress and temperature history effect and illustrated the influence of thermo-mechanical interaction.

In this example the influence of the thermomechanical damage process on the structural behaviour is studied. The example concerns two one-

276

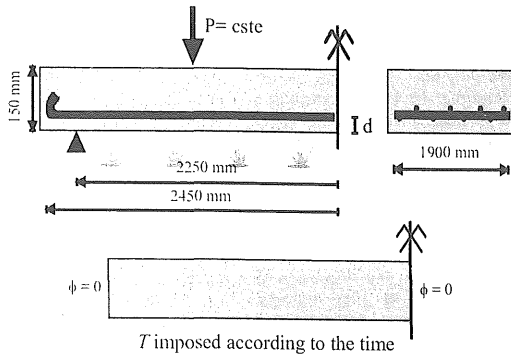### 6.2.3 Simulation of a fire test on a reinforced concrete slab

Figure 9. Geometry and limits conditions of the thermal calculations of the test.

way reinforced concrete slabs, which have been subjected to a fire test (Minne and Vandamme, 1982). The slabs are simply supported on the short sides while the displacements at the other two sides are free. First, the slabs are loaded by two jacks over the full width, then their bottom is heated uniformly. Because of these boundary and loading conditions the slabs could be analysed as beams. The finite element idealization of both slabs, which will be denoted as G1 and G3 in conformity with the experiment, is shown in figure 9. The only difference between the two slabs is the amount of the reinforcement steel and the position, given by the distance d in Table 4, of the bars from the bottom edge of the concrete.

Table 4. Geometry and loading data for reinforced concrete slabs

	Slab G1	Slab G3
d (mm)	15	35
Reinforcement (mm^2)	1178	1414
Line load P (N/mm^2)	5.4	14.6

Eight-noded plane stress elements with eight Gauss integration have been in both analyses. The geometrical data and the loading intensity are listed in Table 4 for both slabs. The values of mechanical properties of the concrete and steel at room temperature are listed in Table 5. Because the dependence of those parameters on the temperature is not given in (Minne

Table 5. Mechanical material properties of concrete and steel

ρ (kg/m^3)	2500
E_0 (N/mm^2)	42.5×10^3
ν	0.2
f_c (N/mm^2)	43.0
f_t (N/mm^2)	2.6
E_s (N/mm^2)	21.5×10^4
f_{sy} (N/mm^2)	504

and Vandamme 1982), the variation is assumed to be identical to the relations that have been proposed by the DTU (Nechnech 2000).

The values of thermal properties of the concrete at room temperature are listed in Table 6. For the same reason as for the mechanical properties, their variations with temperature are assumed to be given by rules proposed by the Eurocode4 (Nechnech 2000). The transient creep coefficients have been assigned to the same values adopted in the previous analysis $\beta_0 = 2.36$ and $\gamma = 0.20$.

Table 6. Thermal properties of concrete slabs

α (°C^{-1})	1.0×10^{-5}
λ ($W/m°C$)	2.2
C ($J/kg°C$)	920

In the first stage of finite element simulations, the heat equation is solved in order to get the temperature distribution in the slabs, while the bottom edge is submitted to an imposed temperature whose variation in time is given by figure 10.
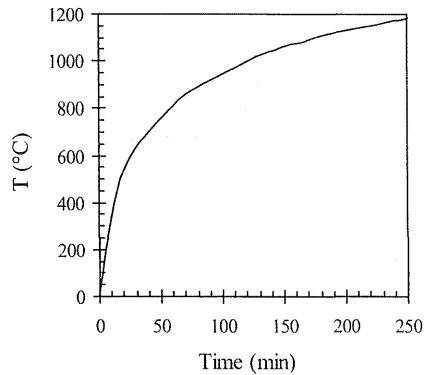

Figure 10. Temperature imposed on the face heated according to the time.

In the mechanical finite element simulations, the temperature gradients and the induced differential thermal strains are imposed, in displacement control, to both the slabs in addition to the external applied load. The confrontation of numerical and experimental results is performed in terms of time-deflection curves as represented in figure11. It is noted that in the experiment the measurements have been terminated when the deflection of the center of the slab exceeded 150 mm for slab G1, while the measurements of slab G3 have been continued until structural failure. The overall agreement with the experimental data is quite reasonable. We observe that slab G3 exhibits a much more ductile behavior than slab G1. This is because the concrete cover of slab G3 is thicker. Consequently, the temperature increase in the reinforcement is postponed leading to a delayed failure. Note that in this analysis the thermo-

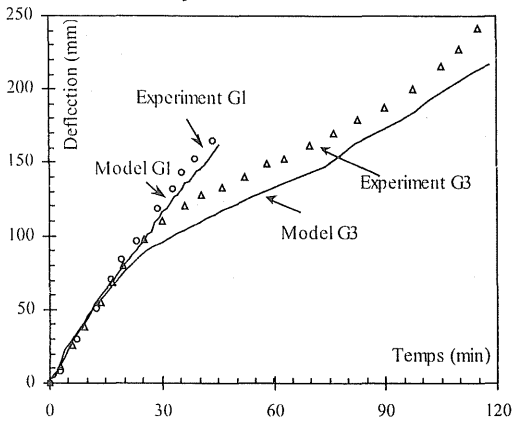mechanical interaction strain term has been considered.

Figure 11. Measured and calculated time-deflection curves for reinforced concrete slabs compared with experimental results

7 CONCLUSION

A model for he nonlinear behavior of concrete under cyclic loading and elevated temperatures has been presented. The model has been shown to predict the correct results for all case of loading, as well as to capture the correct trends in the "sustained stress" problem. Consequently, it can be conclude that the present model can represent accurately the behavior of concrete structures under all thermo-mechanical case of loading.

The equation of the present model result in an ill-posed initial-boundary value problem for material softening. Consequently, uniqueness of solution for the problem is not guaranteed. One result of the ill-posedness is mesh sensitivity in a finite-element analysis. One of the solution is to incorporate an localization limeter. It should be noted that coupling with hydric "pore pressure- shrinkage" is necessary for a better approach of the phenomena.

8 REFERENCES

Anderberg, Y. & Thelandersson, S. 1976. Stress and deformation characteristics of concrete at high temperature:2. Bulletin 54, Lund Institute of Technology, Lund.

Baker, G. & Stabler, J. 1999. Computational modelling of thermally induced fracture in concrete. Proc. Euro-C:530-545.

De Borst, R., & Peeters, P.P.J.M. 1989. Analysis of concrete structures under thermal loading. Comp. Meth. Appl. Mechs. Engng., 77: 293-310.

Feenstra, P.H. 1993. Computational aspects of biaxial stress in plain and reinforceis, and concrete. PhD. Thesis, Delft institute of technology, Netherlands, 149p.

Felicetti, R. & Gambrova P. G. 1998. On the residual properties of high performance Siliceous concrete exposed to high temperature, Mechanics of Quasi-Brittle Materials and Structures, (Dunod edition Paris).

Georgin, J.F. 1998. Contribution à la modélisation du béton sous sollicitation de dynamique rapide - La prise en compte de l'effet de vitesse par la viscoplasticité. PhD. Thesis, INSA de Lyon, France., 204 p.

Gopalaratnam, V.S. & Shah, S.P. 1985. Softening response of plain concrete in direct tension. Journal of American Concrete Institute, 82(3): 310-323.

Heinfling, G. 1998. Contribution à la modélisation numérique du comportement du béton et des structures en béton armé sous sollicitations thermo-mécaniques à hautes températures. PhD thesis, INSA de Lyon, France, 227 p.

Ju, J.W. 1989. On Energy-Based Coupled Elastoplastic Damage Theories: Constitutive Modeling and Computational Aspects. Int. J. Solids Struct., 25(7): 803-833.

Kachanov, L. M. 1985. Time of rupture process under creep conditions. Izvestia Akademii Nauk (in Russian): 26-31.

Kachanov, L. M. 1986. Introduction to continum damage mechanics, Martinus Nijhoff Publishers, Dordrecht, The Netherlands.

Karsan, I. D. & Jirsa, J. O. 1969. Behavior of concrete under compressive loading. J. Struct. Div. ASCE, 95(12): 2535-2563.

Khennane, A. & Baker, G.(1992) Thermo-plasticity models for concrete under varying temperature and biaxial stress. Proc. Royal Soc. Lond. A. 439: 59-80.

Khoury, A.G., Grainger, B.N. & Sullvian, P.J.E. (1985) Transient thermal strain of concrete: Literature review. Conditions within specimen and behavior of individual constituents. Mag. Conc. Res., 37(132), 131-144.

Lee, J. 1998. Theory and implementation of plastic-damage model for concrete structures under cyclic and dynamic loading. Ph.D. thesis, University of California, Berkeley, 151 p.

Mazars, J. 1984. Application de la mécanique de l'endommagement au comportement non linéaire et a la rupture du béton de structure. PhD. Thesis, Université Paris VI, Cachan, France., 283 p.

Meftah, F., Nechnech, W. & Reynouard, J.M. 2000. An elasto-plastic damage model for plain concrete subjected to combined mechanical and high temperatures loads. 14th Engineering Mechanical Conference (A.S.C.E), Austin, U.S.A, 10 p.

Minne, R. & Vandamme, M. 1982. Resistance of reinforced concrete floor slabs against fire (in dutch), Cement 34, 642-646.

Nechnech, W. 2000. Contribution à l'étude numérique du comportement du béton et des structures en béton armé soumises à des sollicitations thermiques et mécaniques couplées - Une approche thermo-élasto-plastique endommageable. PhD. Thesis, INSA de Lyon, France., 222 p.

Nooru-Mohamed, M.B. 1992. Mixed mode fracture of concrete: an experimental approach. PhD .Thesis, Delft University of Technology, 151 p.

Reinhardt, H. W. 1984. Fracture mechanics of an elastic softening material like concrete, Heron, 29 (2): 1-42.

Schneider, U. 1988. Concrete at high temperatures : A general review. Fire Safety Journal, 13: 55-68.